The University of Osaka
Institutional Knowledge Archive

Title	Synthesis of Cu2O nanourchins from Cu nanosheets synthesised in hydrophilic bilayers of hyperswollen lamellar phase
Author(s)	Sasaki, Koki; Miyake, Koji; Uchida, Yoshiaki et al.
Citation	Liquid Crystals. 2023, 50(7-10), p. 1287-1291
Version Type	AM
URL	https://hdl.handle.net/11094/91339
rights	
Note	

The University of Osaka Institutional Knowledge Archive : OUKA

https://ir.library.osaka-u.ac.jp/

The University of Osaka

Synthesis of Cu_2O nanourchins from Cu nanosheets synthesized in hydrophilic bilayers of hyperswollen lamellar phase

Koki Sasaki, Koji Miyake, Yoshiaki Uchida, Norikazu Nishiyama

Graduate School of Engineering Science, Osaka University, Toyonaka, Osaka 560-8531, Japan

E-mail: y.uchida.es@osaka-u.ac.jp

Synthesis of Cu_2O nanourchins from Cu nanosheets synthesized in hydrophilic bilayers of hyperswollen lamellar phase

Nanostructured materials have attracted attention due to their unique chemical and physical properties different from the bulk. Some nanostructures transform their shape through reactions like oxidation and reduction. Here, we report the Cu_2O nanourchin synthesis using spontaneous growth from Cu nanosheets (CuNSs). The CuNSs are synthesized inside the bilayers of the hyperswollen lamellar phase. The obtained CuNSs become Cu_2O after drying at 90°C. Atomic force microscopy indicates that the CuNSs are oxidized in the air in the heating process to give Cu_2O nanourchins.

Keywords: nanosheet; nanourchin; hyperswollen lyotropic lamellar phase; copper (I) oxide

Introduction

Nanostructured materials have attracted attention due to their unique chemical and physical properties different from the bulk: e.g., the high specific surface area of magnesium oxide (MgO) nanoparticles and the high reactivity of titanium dioxide (TiO_2) nanoparticles.[1], [2] Among nanosized materials, metal oxide nanomaterials are used in diverse areas: chemistry, materials science, physics, and biotechnology.[3] The unique electronic structures of nanomaterials determine their conductor, semiconductor, and insulator properties. Copper (I) oxide (Cu_2O) has been studied for its useful optical and electronic properties.[4], [5] Various micro and nanostructures of Cu_2O have been reported: nanocubes, nanooctahedra, nanocages, nanospheres, nanowires, nanourchins, and other highly symmetrical nanostructures.[6]–[11] The Cu_2O nanourchins have excellent properties for various applications due to their high adsorption and catalytic activities.[12] The growth of Cu_2O on low-index copper surfaces is epitaxial with the substrate, and the growth rates of Cu_2O depend on the crystal plane.[13] This method usually gives nanourchins consisting of Cu and Cu_2O because oxidation occurs on the

surfaces. We expected that we could synthesize Cu_2O nanourchins from Cu nanosheets (CuNSs) composed of small crystallites only with surface regions, as shown in Figure 1.

We have recently developed a method to synthesize NSs by using several-nm-thick bilayers in hyperswollen lamellar (HL) phases as a reaction field.[14], [15] We named this method the 'two-dimensional reactors in amphiphilic phases (TRAP)' method.[16]–[18] The TRAPs prevent NSs from aggregating because they keep several hundred nm intervals from each other. This method gives a suspension of free-standing NSs with several nm thicknesses. The TRAP method can control the size of NSs by changing the shear stress and composition of the HL phase solution; they decide the bilayer width and thickness.[18] - [20] The NSs are composed of small crystallites with random orientations. Here, we report the synthesis method of Cu_2O nanourchins from CuNSs. We discuss the growth mechanism of Cu_2O nanourchins using atomic force microscopy (AFM), transmission electron microscopy (TEM), and X-ray diffraction (XRD) measurements.

Experimental

Synthesis of Cu_2O nanosheets

Solvents and reagents were reagent-grade and used without further purification. The heptane solution (21 mL) of copper(II) nitrate trihydrate ($Cu(NO_3)_2 \cdot 3H_2O$) (1.0×10^{-1} wt%), Brij L4 (6.9 wt%), water (1.9 wt%), and methanol (1.0 wt%) and the heptane solution (21 mL) of $NaBH_4$ (2.6×10^{-2} wt%), Brij L4 (6.9 wt%), sodium hydroxide solution (pH 11) (1.9 wt%), and methanol (1.0 wt%) were separately prepared. The TRAP solution dissolving $NaBH_4$ was poured into the TRAP solution dissolving $Cu(NO_3)_2$ under stirring (300 rpm). The final products were centrifuged at 11000 rpm for 30 min, washed three times with ethanol and dried at 90°C in the air.

Synthesis of Cu_2O@Cu fine particles

Solvents and reagents were reagent-grade and used without further purification. The heptane solution (42 mL) of $Cu(NO_3)_2 \cdot 3H_2O$ (1.1×10^{-1} wt%), water (2.0 wt%), and methanol (1.1 wt%) and the heptane solution (42 mL) of $NaBH_4$ (3.6×10^{-2} wt%), sodium hydroxide solution (pH 11) (2.0 wt%), and methanol (1.1 wt%) were separately prepared. The heptane solution dissolving $NaBH_4$ was poured into the heptane solution dissolving $Cu(NO_3)_2$ under stirring (300 rpm). The final products were centrifuged at 11000 rpm for 30 min, washed three times with ethanol and dried at 90°C in the air.

Results and discussion

We examined the effect of the ingredients of CuNSs on the stability of the HL phase. We can confirm the stability of the HL phase by observing its birefringence using a polarizing film wrapped around the vessel because the birefringence reflects the stability of the HL phases, as shown in Figure 2a.[18] The polarized photograph of the TRAP solution consisting of heptane (90.1 wt%), Brij L4 (6.9 wt%), a mixture containing tetraethylene glycol monododecyl ether ($C_{12}E_4$) as the main component, water (1.9 wt%), and methanol (1.0 wt%) shows birefringence typical of HL phases, as shown in Figure 2b. The upper half of the vessel is empty, and the lower half contains the solution. We separately added copper(II) nitrate ($Cu(NO_3)_2$) and sodium borohydride ($NaBH_4$) to the TRAP solutions in two vessels. The polarized photographs of the two TRAP solutions show birefringence, as shown in Figures 2c and 2d.[17]–[19] Since we cannot track the composition in the bilayers dynamically, the formation of nanosheets has proved the trapping of the hydrophilic ingredients inside the bilayers.[19] These results indicate that $Cu(NO_3)_2$ and $NaBH_4$ are trapped in the hydrophilic TRAPs and that their addition did not destabilize the HL phases.

Then, we tried synthesizing CuNSs by pouring the TRAP solution dissolving $NaBH_4$ into the TRAP solution dissolving $Cu(NO_3)_2$. After stirring the mixed TRAP solution for 15 minutes, we centrifuged the reaction mixture to give a black precipitate. We washed the black precipitate three times with ethanol and dried it at 90°C in the air. The X-ray diffraction (XRD) pattern of the black powder has several peaks typical of Cu_2O, as shown in Figure 3a.[21] Meanwhile, the XRD pattern of the fine particles, synthesized in the heptane solution without Brij L4, has the peaks typical of both Cu and Cu_2O. These results indicate that the black powder becomes Cu_2O from metallic Cu. This transformation should come from the excess amount of $NaBH_4$.[21] The obtained black powder seems easily oxidized because of its high specific surface area and small internal volume. We measured the horizontal width and thickness of the products before drying by atomic force microscopy (AFM) as 908 ± 120 nm and 0.57 ± 0.11 nm, respectively, as shown in Figure 3b. However, the horizontal width and thickness of the dried products become 347 ± 93 nm and 102 ± 35 nm, respectively, as shown in Figure 3c. These results indicate that the drying induces deformation. Some of the deformed particles include a wired structure. To confirm the shape of the dried products, we performed transmission electron microscopy (TEM). The TEM photographs show sea urchin-like particles, as shown in Figure 3d. We can determine the crystal structure using selected area electron diffraction (SAED) patterns from the Bragg reflection of the electron beam corresponding to the crystal structures. The SAED measurement of the particles gives the same patterns as Cu_2O.[22] When the Cu_2O nanourchins were polycrystals, the SAED patterns would be a ring. Therefore, the concentric circles of the SAED patterns indicate that the sea urchin-like particles are composed of small crystallites with random orientation. We can conclude that the Cu_2O nanourchins grew from CuNSs.

Conclusion

We have found the growth of Cu_2O nanourchins from CuNSs synthesized in the hydrophilic TRAPs. We conclude that the CuNSs deform in the oxidation process to Cu_2O nanourchins.

Acknowledgements

This work was supported in part by the Advanced Characterization Nanotechnology Platform, Nanotechnology Platform Program of the Ministry of Education, Culture, Sports, Science and Technology (MEXT), Japan, Grant Number JPMXP09A21OS0028 at the Research Center for Ultra-High Voltage Electron Microscopy (Nanotechnology Open Facilities) in Osaka University, and JSPS KAKENHI Grant Number JP22H04477 and JP22J10688.

References

[1] Bindhu MR, Umadevi M, Micheal MK, Arasu MV, Al-Dhabi NA. Structural, morphological and optical properties of MgO nanoparticles for antibacterial applications. Mater. Lett. 2016;166:19–22.

[2] Ota M, Dwijaya B, Hirota Y, Uchida Y, Tanaka S, Nishiyama N. Synthesis of Amorphous TiO_2 Nanoparticles with a High Surface Area and Their Transformation to $Li_4Ti_5O_{12}$ Nanoparticles. Chem. Lett. 2016;45(11):1285–1287.

[3] Yoon Y, Truong PL, Lee D, Ko SH. Metal-Oxide Nanomaterials Synthesis and Applications in Flexible and Wearable Sensors. ACS Nanosci. Au. 2022;2(2):64–92.

[4] Heinemann M, Eifert B, Heiliger C. Band structure and phase stability of the copper oxides Cu_2O, CuO, and Cu_4O_3. Phys. Rev. B. 2012;87(11):115111.

[5] Zhou T, Zang Z, Wei J, Zheng J, Hao J, Ling F, Tang X, Fang L, Zhou M. Efficient charge carrier separation and excellent visible light photoresponse in Cu_2O nanowires. Nano Energy. 2018;50:118–125.

[6] Luo F, Wu D, Gao L, Lian S, Wang E, Kang Z, Lan Y, Xu L. Shape-controlled synthesis of Cu_2O nanocrystals assisted by Triton X-100. J. Cryst. Growth. 2005;285(4):534–540.

[7] Xu H, Wang W, Zhu W. Shape Evolution and Size-Controllable Synthesis of Cu_2O Octahedra and Their Morphology-Dependent Photocatalytic Properties. J. Phys. Chem. B. 2006;110(28):13829–13834.

[8] Lu C, Qi L, Yang J, Wang X, Zhang D, Xie J, Ma J. One-Pot Synthesis of Octahedral Cu_2O Nanocages via a Catalytic Solution Route. Adv. Mater. 2005;17(21):2562–2567.

[9] Zhang J, Liu J, Peng Q, Wang X, Li Y. Nearly Monodisperse Cu_2O and CuO Nanospheres: Preparation and Applications for Sensitive Gas Sensors. Chem. Mater. 2006;18(4):867–871.

[10] Wang W, Varghese OK, Ruan C, Paulose M, Grimes CA. Synthesis of CuO and Cu_2O crystalline nanowires using $Cu(OH)_2$ nanowire templates. J. Mater. Res. 2003;18(12):2756–2759.

[11] He J, Jiang Y, Peng J, Li C, Yan B, Wang X. Fast synthesis of hierarchical cuprous oxide for nonenzymatic glucose biosensors with enhanced sensitivity. J. Mater. Sci. 2016;51(21):9696–9704.

[12] Mao BG, Chu DQ, Wang LM, Wang AX, Wen YJ, Yang XZ. Ultrasound-assisted synthesis of sea urchin-like Cu_2O architectures. Mater. Lett. 2013;109:62–65.

[13] Gattinoni C, Michaelides A. Atomistic details of oxide surfaces and surface oxidation: the example of copper and its oxides. Surf. Sci. Rep. 2015;70(3):424–447.

[14] Larche FC, Appell J, Porte G, Bassereau P, Marignan J. Extreme Swelling of a Lyotropic Lamellar Liquid Crystal. Phys. Rev. Lett. 1986;56(16): 1700–1703.

[15] Strey R, Schomäcker R, Roux D, Nallet F, Olsson U. Dilute Lamellar and L_3 Phases in the Binary Water-$C_{12}E_5$ System. J. Chem. Soc. Faraday Trans. 1990;86(12):2253–2261.

[16] Uchida Y, Nishizawa T, Omiya T, Hirota Y, Nishiyama N. Nanosheet Formation in Hyperswollen Lyotropic Lamellar Phases. J. Am. Chem. Soc. 2016;138(4):1103–1105.

[17] Sasaki K, Gaitan JAH, Okue T, Matoba S, Tokuda Y, Miyake K, Uchida Y, Nishiyama N. Amorphous Aluminosilicate Nanosheets as Universal Precursors for the Synthesis of Diverse Zeolite Nanosheets for Polymer-Cracking Reactions. Angew. Chem. Int. Ed. 2022;61(46):e202213773.

[18] Sasaki K, Gaitan JAH, Tokuda Y, Miyake K, Uchida Y, Nishiyama N. A nanosheet molding method to estimate the size of bilayers suspended in liquids. J. Mater. Chem. C. 2022;10(42):15816–15821.

[19] Sasaki K, Miyake K, Uchida Y, Nishiyama N. Mechanochemical Synthesis of Dispersible Platinum Nanosheets for Enhanced Catalysis in a Microreactor. ACS Appl. Nano Mater. 2022;5(4):4998–5005.

[20] Yamamoto J, Tanaka H. Shear Effects on Layer Undulation Fluctuations of a Hyperswollen Lamellar Phase. Phys. Rev. Lett. 1995;74(6):932–935.

[21] Liu QM, Zhou DB, Yamamoto Y, Ichino R, Okido M. Preparation of Cu nanoparticles with $NaBH_4$ by aqueous reduction method. Trans. Nonferrous Met. Soc. China. 2012;22(1):117–123.

[22] Mallik M, Monia S, Gupta M, Ghosh A, Toppo MP, Roy H. Synthesis and characterization of Cu_2O nanoparticles. J. Alloys Compd. 2020;829:154623.

Figure 1. Schematic illustration of the growth mechanism of Cu_2O nanourchins from CuNSs. The Cu_2O grows on copper surfaces epitaxially.

Figure 2. Observation of birefringence of the heptane solution of Brij L4 containing water. (a) The optical system to take polarized photographs of hyperswollen lamellar phases. A polarizing film is wrapped around a vessel while tilted at 45°. Polarized photographs of (b) TRAP solution of heptane (90.1 wt%), water (1.9 wt%), Brij L4 (6.9 wt%) and methanol (1.0 wt%), (c) TRAP solution of heptane (90.1 wt%), water (1.9 wt%), Brij L4 (6.9 wt%), methanol (1.0 wt%) and $Cu(NO_3)_2$ (1.0×10^{-1} wt%), and (d) TRAP solution of heptane (90.2 wt%), sodium hydroxide solution (pH 11) (1.9 wt%), Brij L4 (6.9 wt%), methanol (1.0 wt%), and $NaBH_4$ (2.7×10^{-2} wt%).

Figure 3. Characterization of CuNSs. (a) XRD patterns of Cu_2O nanourchins that grew from the CuNSs (red) and Cu fine particles (blue) and standard XRD patterns of Cu and Cu_2O (black). AFM photograph and cross-section of one of the synthesized CuNSs (b) before and (c) after drying. (d) TEM photograph of Cu_2O nanourchins that grew from CuNSs, and SAED pattern of CuNSs.

Figure 1.

Figure 2.

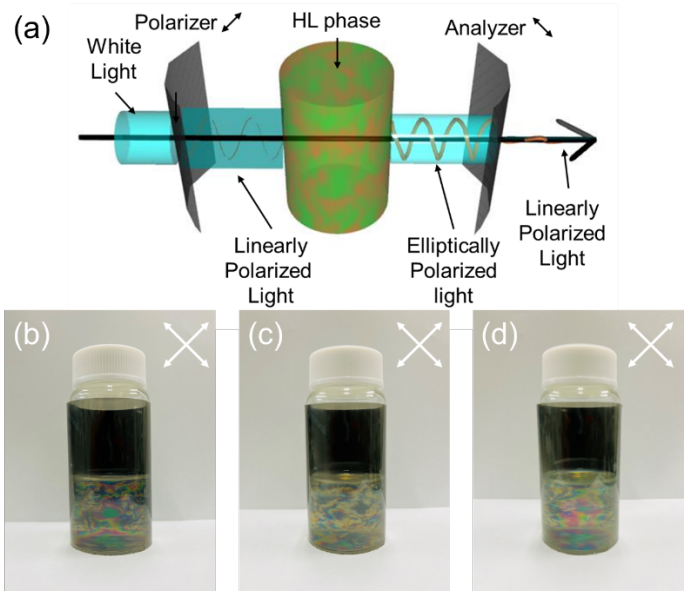
(a)
Polarizer
HL phase
Analyzer
White Light
Linearly Polarized Light
Elliptically Polarized light
Linearly Polarized Light
(b)
(c)
(d)

Figure 3.

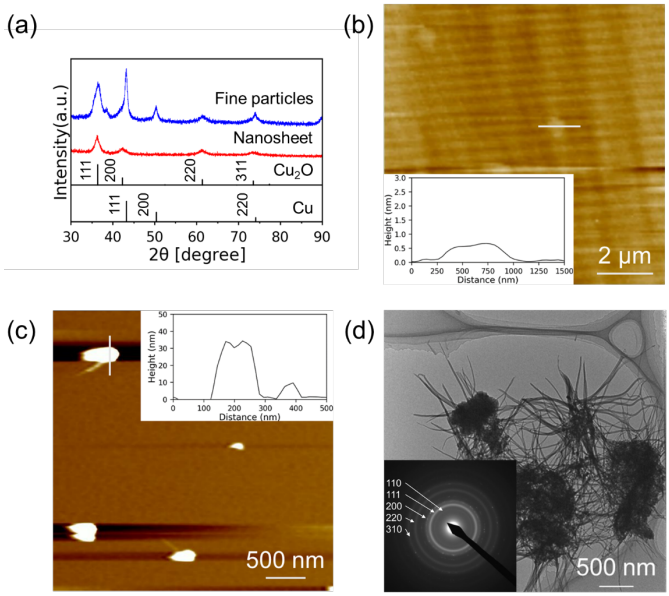
(a)
Fine particles
Nanosheet
Intensity(a.u.)
111
200
220
311
Cu2O
111
200
220
Cu
30
40
50
60
70
80
90
2θ [degree]
(b)
Height (nm)
Distance (nm)
2 μm
(c)
Height (nm)
Distance (nm)
500 nm
(d)
110
111
200
220
310
500 nm